MONOTONIC AND CYCLIC PLASTICITY MODEL FOR CLAY

Nagoya Institute of Technology Student Member Chowdhury E. Q.
Nagoya Institute of Technology Member Nakai T.

ABSTRACT

It's long way back when an isotropic hardening clay model based on the modified stress t_{ij} was proposed. The amazing features of that model were the introduction of modified stress tensor t_{ij} based on the 'Spatial mobilized plane (SMP)' concept and the decomposition of plastic strain increments into two components. By the former it was possible to recognized the effect of intermediate principal stress (triaxial compression, extension and true triaxial conditions) on the stress-dilatancy and the strength of clay and the later was to consider the effect of stress path on the direction of plastic flow. More specifically, it was assumed that part of the plastic strain increment satisfy flow rule and the remaining part was produced due to the increase of normal stress (t_N). By this hypothesis it was possible to distinguish the stress-dilatancies under shear at constant mean principal stress, constant radial stress or the plane strain conditions. This model was called t_{ij}-clay model[3] and could realistically predict the stress-strain behavior and the strength of normally consolidated clay.

However, likewise other isotropic hardening clay models, this model could not predict the behavior of clay under repeated loading or shearing of previously overconsolidated clay. Kinematic hardening models are usually employed to express the behavior under cyclic loading. On a later occasion kinematic extension of the above mentioned isotropic hardening model named kinematic t_{ij}-clay model[4] was proposed. Even though kinematic model, it failed to anticipate the behavior of overconsolidated clay or repeatedly loaded clay. Because, both stress-dilatancy and strength characteristics of overconsolidated clay changes substantially and the magnitudes of strains drastically reduces with the overconsolidation. Also, overconsolidated clay shows hardening and softening, positive and negative dilatancy. Considering these flaws of the original kinematic t_{ij}-clay model, a new kinematic t_{ij}-clay model has been proposed which, to some extent can simulate all the above mentioned features. Moreover, this model behaves exactly in the same way as the previous models for normally consolidated clay. Finally triaxial test results of the reconstituted Fujinomori clay and corresponding analyses have been presented to demonstrate the validity of the new model.

BRIEF BACKGROUND

Flaws of the well known Cam-clay model, for instance path dependency of the flow rule and the strength of clay forced the authors of the references 1, 2 and 3 to think in a different way based on the assumption that there must exist a plane on which stress ratio and strain increment ratio would have a unique relation. Later, they found a plane and termed it as "Spatial Mobilized Plane (SMP)". A more general interpretation of the "SMP" was given by Nakai et. al.[3] by introducing modified stress tensor t_{ij}. The modified stress tensor, t_{ij} is coaxial and evolved from the stress tensor σ_{ij} as given below.

$$t_{ij} = \sigma_{ik} a_{kj} \qquad (1)$$

Where, a_{ij} are the direction cosines of the SMP and is given by equation 2.

$$a_{ij} = \sqrt{\frac{J_3}{J_2}} r_{ij}^{-1} = \sqrt{\frac{J_3}{J_2}} \left(\sigma_{ik} + I_2 \delta_{ik}\right)\left(I_1 \sigma_{kj} + I_3 \delta_{kj}\right)^{-1} \qquad (2)$$

r_{ij} of the above equation is one half power of the stress tensor σ_{ij}, such that $\sigma_{ij} = r_{ik} r_{kj}$. J_2 and J_3 are the second and third invariants of stress tensor σ_{ij} and I_1, I_2 and I_3 are the first, second and third invariants of the tensor r_{ij}.

Once the modified stress tensor t_{ij} is known, normal and parallel components of the modified stress on the SMP and the stress ratio can be calculated as follows:

$$t_N = t_{ij} a_{ij} \qquad (3) \qquad t_S = \sqrt{t'_{ij} t'_{ij}} \qquad (4) \qquad X = {}^{t_S}\!/_{t_N} = \sqrt{x_{ij} x_{ij}} \qquad (5)$$

where, $t'_{ij} = t_{ij} - t_N a_{ij}$ (7) and $x_{ij} = {t'_{ij}}/{t_N}$ (8)

Similarly, normal and parallel components of the strains on the SMP are

$d\varepsilon_{SMP^*} = d\varepsilon_{ij} a_{ij}$ (10) and $d\gamma_{SMP^*} = \sqrt{d\varepsilon'_{ij} d\varepsilon'_{ij}}$ (11) where $d\varepsilon'_{ij} = d\varepsilon_{ij} - d\varepsilon_{SMP^*} a_{ij}$ (12)

strain increment ratio on the SMP is $Y = {d\varepsilon_{SMP^*}}/{d\gamma_{SMP^*}}$. (13)

Stress-dilatancy plots (using X and Y) of various triaxial tests on the reconstituted Fujinomori clay under constant mean principal stress showed a unique straight line relation independent of the intermediate principal stress. It is assumed that part of the total plastic strain increment satisfy flow rule and the remaining part has been linked to the increase of normal stress t_N, forced the test results under varying mean principal stress to follow the same stress-dilatancy relation. The above mentioned stress-dilatancy relation is given by equation 14.

$$Y = \frac{X_f - X}{\alpha} + Y_f = \frac{1}{\alpha}\left(M^* - X\right) \qquad (14)$$

Where, X_f and Y_f are the failure stress ratio and strain increment ratio respectively and $M^* = X_f + \alpha Y_f$. Stress-dilatancy relation using Cam-clay parameters showed varying tendency depending on the intermediate principal stress and the stress path. Matsuoka-Nakai also characterized the failure of a soil element as $X_f = cons.$, known as Matsuoka-Nakai failure criteria showed close agreement with the observed strength under triaxial compression, extension and true triaxial stress conditions.

Using above stress-dilatancy relation and assuming associated flow rule, yield (f) and plastic potential (g) functions, can be derived as eq. 15.

$$f \equiv g = ln\, t_N + \frac{-\alpha}{1-\alpha} ln \left|1 - (1-\alpha)\frac{X}{M^*}\right| - ln\, t_{N1} = 0 \qquad (15)$$

Now, total strain increment for any arbitrary stress increment has been given as follows:

$$d\varepsilon_{ij} = d\varepsilon^e_{ij} + d\varepsilon^p_{ij} = d\varepsilon^e_{ij} + d\varepsilon^{p(IC)}_{ij} + d\varepsilon^{p(FR)}_{ij} \qquad (16)$$

Elastic strain increment was given by Hook's law

$$d\varepsilon^e_{ij} = \frac{1+\nu_e}{E_e} d\sigma_{ij} - \delta_{ij}\frac{\nu_e}{E_e} d\sigma_{kk} \qquad (17) \qquad E_e = \frac{3(1+\nu_e)(1+e_0)p}{\varkappa} \qquad (18)$$

Plastic strain increment compressive isotropically and satisfying flow rule were as follows:

$$d\varepsilon^{p(IC)}_{ij} = \frac{\delta_{ij}}{3} K\langle dt_N \rangle \qquad (19) \qquad K = \frac{\lambda - \varkappa}{1+e_o}\frac{1}{t_N}\frac{t_N}{t_{N1}} \qquad (20)$$

$$d\varepsilon^{p(FR)}_{ij} = \Lambda\frac{\partial g}{\partial t_{ij}} = \Lambda\frac{\partial f}{\partial t_{ij}} \qquad (21) \qquad \Lambda = \frac{\dfrac{\partial f}{\partial \sigma_{pq}} d\sigma_{pq} - K\langle dt_N \rangle}{\dfrac{\partial g}{\partial t_{mm}}} \quad \frac{\dfrac{\partial f}{\partial \sigma_{pq}} d\sigma_{pq} - K\langle dt_N \rangle}{\dfrac{\partial f}{\partial t_{mm}}} \qquad (21)$$

The model described above is the isotropic hardening t_{ij}-clay model[3], which gives realistic stress

strain response and strength of clay under monotonic or proportional loading conditions. This model was extended to a kinematic model (named kinematic t_{ij}-clay model[4]) by simply assuming that the yield surface moves in the stress ratio space by satisfying the following condition.

$$X^* = \sqrt{x^*_{ij} x^*_{ij}} = \sqrt{(x_{ij} - n_{ij})(x_{ij} - n_{ij})} = \xi = cons. \tag{22}$$

ξ is a soil parameter and n_{ij} is the stress ratio of the center of the yield surface and assumed to move to a new position due to the change of stress ratio as eq. 23.

$$n_{ij}(new) = n_{ij}(old) + dn_{ij} = n_{ij}(old) + k dx_{ij} \tag{23}$$

k can be calculated from the compatibility condition of eq. 22. To be consistent with the above translation rule, yield and plastic potential of equation 15 was modified as bellow.

$$f \equiv g = ln\, t_N + \frac{-\alpha}{1-\alpha} ln \left| 1 - (1-\alpha)\frac{X^* + n}{M^*} \right| - ln\, t_{N1} = 0 \tag{24}$$

where scalar n is given by $n = \sqrt{n_{ij} n_{ij}}$ (25)

The rest remains the same as isotropic hardening t_{ij}-clay model. Though kinematic, this model extremely over predicted strains under cyclic loading as it uses the same hardening function as t_{ij}-clay model also relative proportion of the normal component of the strains was over predicted during cyclic loading due to the use of same stress-dilatancy relation as normally consolidated clay.

NEW MODEL OUTLINE

Kinematic models are supposed to express stress induced anisotropy such as cyclic loading, from this point of view above mentioned model was a kinematic one. But no attempt has been made to consider some common features usually observed during cyclic loading. In the present model (kinematic t_{ij}-clay model, ver.4), these features are considered in a simplified way, while on the other hand it behaves exactly in the same way as the isotropic hardening t_{ij}-clay model for normally consolidated clay under monotonic and proportional loading paths.

It is usually observed that the stress-dilatancy relation of the over consolidated clay or the stress-dilatancies of successive cycles of loading during cyclic triaxial tests changes substantially. Which is evident in figures 4(d) and 5(d). Where, plots show observed response and dashed line show the stress-dilatancy proposed by equation 14. It is difficult to determine experimentally a changing pattern of the stress-dilatancy, because, during cyclic loading magnitude of plastic strains reduces drastically and elastic parts comprises significant part of the total strain increment. Considering this difficulty and observing from figures 4(d) and 5(d) that the relative proportion of the normal strain component reduces during second cycle of loading, we intuitively modified the equation of the plastic potential (g) as follows:

$$g = ln\, t_N + \frac{1}{G^l} \frac{-\alpha}{1-\alpha} ln \left| 1 - (1-\alpha)\frac{X^* + n}{M^*} \right| \tag{26}$$

where, G is a function of over consolidation $(0 < G \leq 1)$ based on the t_{ij} stress parameters. Detail expressions for G will be given subsequently. The implication of the above plastic potential is that for over consolidated (either normally or due to cyclic loading) clay it is flatter than normally consolidated one, thus indicates a larger proportion of shearing strain component in the over consolidated clay than normally consolidated.

Yield function (f) is given in the same way as the previous kinematic model (as in eq. 24), thus utilizes non-associated flow rule in general but becomes associated flow for normally consolidated clay. For being non-associated flow, chances of plastic instability arises when stress increment lies between the tangents to the yield and plastic potentials, because second order plastic work increment becomes negative $d(dW^p) = d\varepsilon^p_{ij} d\sigma_{ij} < 0$ (angle between stress increment vector and strain increment vector >90°). Apart from the ordinary elastoplastic models this model assumes plastic strain increment to be composed of two components, so, even if the flow rule component of strain

increment produce negative second order work increment the remaining part must be positive and may be positive as a whole. Numerically it has been verified that total second order work increments are positive for many different stress paths.

The second fact that observed in the triaxial tests is that plastic strain increment reduces drastically in over consolidated clay. Magnitude of plastic strain increment is governed by the hardening function and in clay, hardening function is given by the straight line relation of ε_v^p vs. lnp (or v vs. lnp).

i.e. $$d\varepsilon_v^p = \frac{\lambda-\varkappa}{1+e_0}\frac{dp}{p} \equiv \frac{\lambda-\varkappa}{1+e_0}\frac{dt_N}{t_N} \qquad (27)$$

To fit the above mentioned fact in the hardening function, we modify above hardening rule as in the following equation:

$$d\varepsilon_v^p = G^m \frac{\lambda-\varkappa}{1+e_0}\frac{dt_N}{t_N} \qquad (28)$$

Thus, the amount of plastic strain increment for over consolidated clay will be less than normally clay, since $G<1$ for over consolidated clay.

The third modification that has been made by treating the expression of Λ of equation 21 as follows:

$$\Lambda = \frac{\frac{\partial f}{\partial \sigma_{pq}} d\sigma_{pq} - K\langle dt_N \rangle}{\frac{\partial g}{\partial t_{mm}} - a\frac{\ln G}{t_N}} \qquad (29)$$

Denominator of the above expression of Λ has been modified intuitively as Hashiguchi's subloading surface model[8]. Above expression of Λ has got many implications. Firstly, for over consolidated clay denominator of equation 29 will be larger than that of equation 21, thus reduces the magnitude of strains. Secondly, it forces positive dilatancy to occur during hardening phase. While on the other hand in Cam-clay or in t_{ij}-clay models, positive dilatancy and softening occurs simultaneously. Thirdly, it increase the strength of over consolidated clay. For normally consolidated clay, second term of the denominator of Λ vanishes and the above equation becomes exactly the same as equation 21.

Modifications made so far by using G. Now referring to figures 1(a) and 1(b) we define G as follows:

$$G = \frac{t_{N3}}{t_{N1e}} \qquad (30) \qquad t_{N3} = \frac{t_{N1}+t_{N2}}{2} + R\frac{t_{N1}-t_{N2}}{2} \qquad (31)$$

$$R = \frac{x_{ij}^* n_{ij}}{\|x^*\|\|n\|} \qquad (32) \qquad \text{and} \qquad t_{1Ne} = t_{N0}\exp\left\{\frac{\varepsilon_{v(2)}^p}{\frac{\lambda-\varkappa}{1+e_0}}\right\} \qquad (33)$$

Hill's loading criteria has been used as to judge yielding as in equation 34.

$$\left.\begin{array}{lll} \textit{loading}: & f=0 \quad \textit{and} & \frac{\partial f}{\partial \sigma_{ij}} E_{ijkl} d\varepsilon_{kl} \geq 0 \\ \textit{Unloading}: & f<0 \quad \textit{or} & \frac{\partial f}{\partial \sigma_{ij}} E_{ijkl} d\varepsilon_{kl} < 0 \end{array}\right\} \qquad (34)$$

MODEL VERIFICATION

Soil parameters used in the analyses are listed in table-1. C_t, C_e, R_f, α, ν were introduced in the t_{ij}-clay model[3] and ξ was introduced in original kinematic t_{ij}-clay model[4]. Methods to determine theseparameters were explained in references 3 and 4. Parameters a, l and m are introduced in the present model and are to be determined by trial analyses of a cyclic triaxial test.

Triaxial compression and extension test paths (test 1 and 2) are shown in figures 2(a) and 3(a) respectively. Figures 2(b) and 3(b) show stress ratio (q/p') vs. axial strain (ε_a) vs. volumetric (ε_v) strain responses. These two figures show that the response observed by all t_{ij} models are the same also predicted strengths are close to the observed ones. On the other hand original Cam-clay closely predicts the strength in case of triaxial compression but extremely over predicts in triaxial extension. This is the superiority of t_{ij} models over ordinary models. Also both model slightly over predicted volumetric strains, observed volumetric strains were a little less due to the aging effect.

Two simple cyclic triaxial tests (test 3 & 4) has been carried out to observe various aspects of clay response, test paths are shown in figures 4(a) and 5(a). Strain rate was sufficiently low to ensure drainage. Figures 4(b), 5(b), and 4(c) and 5(c) show stress ratio vs. axial strain (ε_a) and volumetric (ε_v) strain responses respectively. t_{ij}-clay and Cam-clay models show completely elastic response during second cycle of loading and hence are not suitable for cyclic loading. On the other hand original kinematic t_{ij}-clay model over predicts volumetric strains. Also, it shows weaker response soon after the transition from elastic to elastoplastic condition in second part of loading. Present model (kinematic t_{ij}-clay model, ver.4), closely predicted the volumetric strains and stronger responses were observed after transition from elastic to elastoplastic condition. Present model also predicts higher strength than normally consolidated clay and matches observed tendency. Also, it shows positive dilatancy or softening phase at the final stage of shearing. But, all other models don't have such capability.

Variable amplitude of shear loading were applied in test 5 as shown in figure 6(a). Present model response shows stronger shearing resistance and higher strength than the original kinematic t_{ij}-clay model. Also, volumetric strain has been closely predicted.

In another constant amplitude cyclic triaxial test which is not presented here for space limitation, showed volumetric strain in successive cycles reduces rapidly and at one stage almost no volumetric strain occurs. In that case too, present model shows reduction or stabilization of volumetric strain but has not ceased completely.

COMMENTS

A normally consolidated clay looses it's properties due to over consolidation by isotropic or by repeated loading. Since, it is difficult to determine the properties of over consolidated clay we tried to view this complexity by simple functions of over consolidation ratio. Various modifications have been made, though some of them are not supported by the presently accepted concepts of plasticity. Modifications have been made rather superficially than considering them in the derivation process of yield and plastic potential functions, determination of Λ or hardening functions.

REFERENCES

1) Matsuoka, H. and Nakai, T. (1974): "Stress-deformation and strength characteristics of soil under three different principal stresses," Proc., JSCE, No. 232, pp. 59-70
2) Nakai, T. and Matsuoka, H. (1983): "Shear behavior of sand and clay under three-dimensional stress condition," Soils and Foundations, Vol. 23, No.2, pp. 26-42
3) Nakai, T. and Matsuoka, H. (1986): "A generalized elastoplastic constitutive model for clay in three dimensional stresses, "Soils and Foundations, Vol.26, No. 3, pp. 81-98
4) Nakai, T. and Hoshikawa, T. (1991): "Kinematic hardening model for clay in three dimensional stresses," Proc. 7th. Int. Conf. Comp. Meth. Adv. Geom., (1), pp. 655-660
5) Nakai, T., Hoshikawa, T. and Chowdhury, E. Q. (1995): "Stress-strain behavior of clay under cyclic loading and it's modeling," Ist. Int. Conf. on Earthquake geotech. Engg., IS- TOKYO '95, vol. 1, pp. 405-410
6) Asaoka, A., Nakano, M. and Noda, T. (1994): "Soil-water coupled behavior of clay near/ at critical state," Soils and Foundations, Vol. 34, No. 1, pp. 91-105
7) Hashiguchi, K. (1980): "Constitutive equations of elastoplastic materials with elastic-plastic transition," J. Appl. Mech., ASME, Vol.47, No.2, pp. 266-272
8) Hashiguchi, K. (1989): "Subloading surface model in unconventional plasticity," International Journal of Solid Structure, Vol.25, No.4, pp. 57-70
9) Hashiguchi, K. (1994): "On the loading criterion," International Journal of Plasticity, Vol.10, No.8, pp 871-878

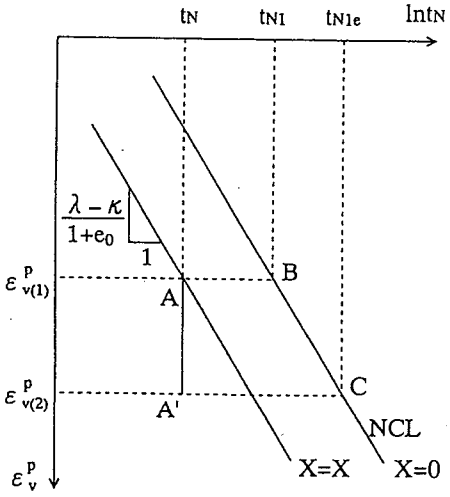

Fig 1(a): Definition of t_{N1} and t_{N1e} in ε_v^p vs. $\ln t_N$ plane

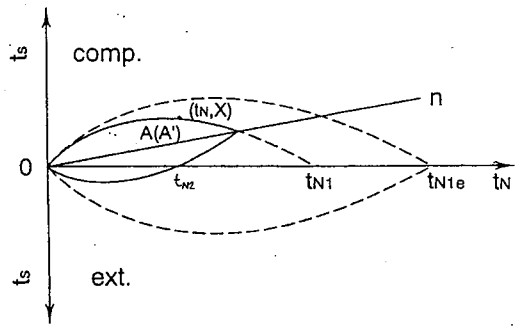

Fig 1(b):Definition of t_{N1}, t_{N2} and t_{N1e} in t_S vs. t_N plane

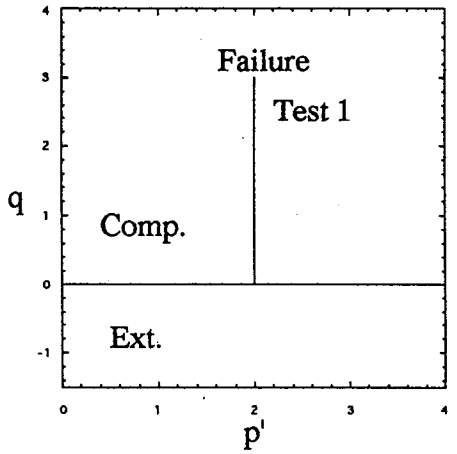

Fig 2(a): Stress path of test 1

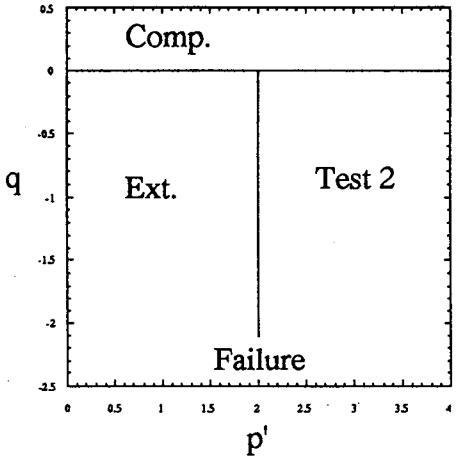

Fig 3(a): Stress path of test 2

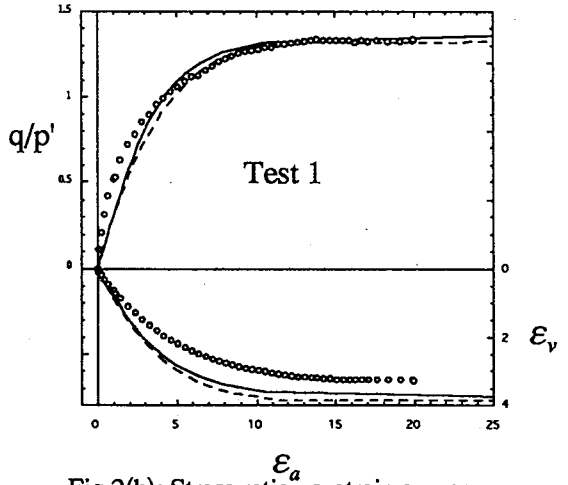

Fig 2(b): Stress ratio vs. strain curves

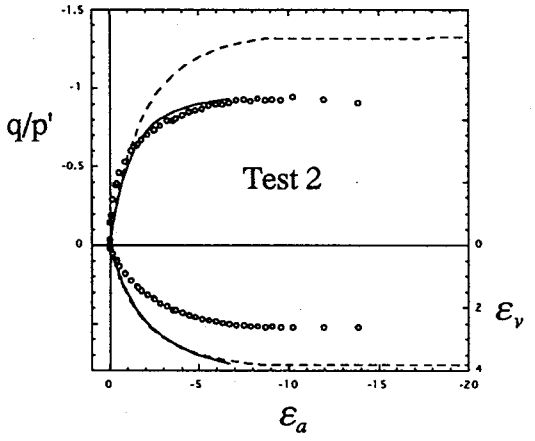

Fig 3(b): Stress ratio vs. strain curves

Legend

o	Observed
— — -	Cam-clay model
———	All t_{ij}-clay models

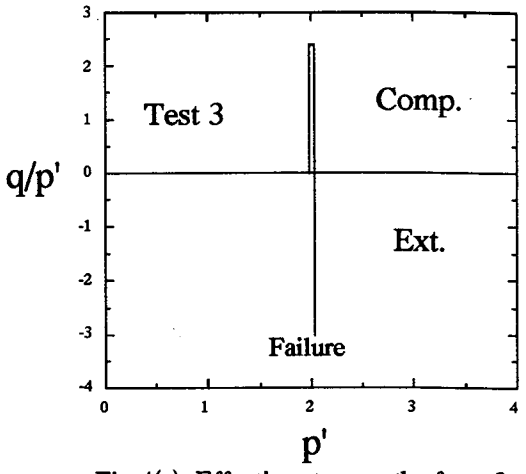

Fig 4(a): Effective stress path of test 3

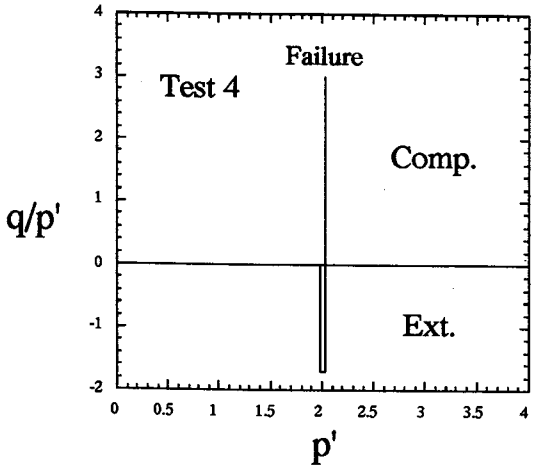

Fig 5(a): Effective stress path of test 4

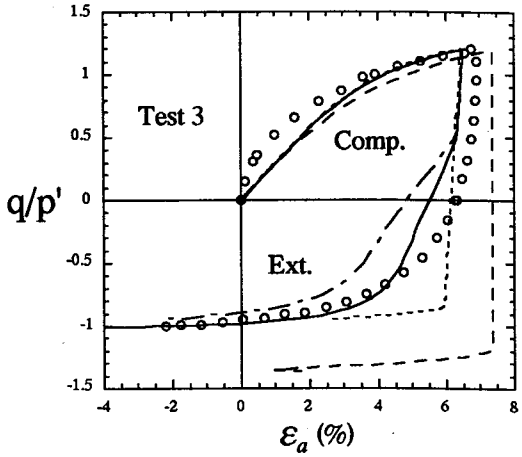

Fig 4(b): Stress ratio vs. axial strain

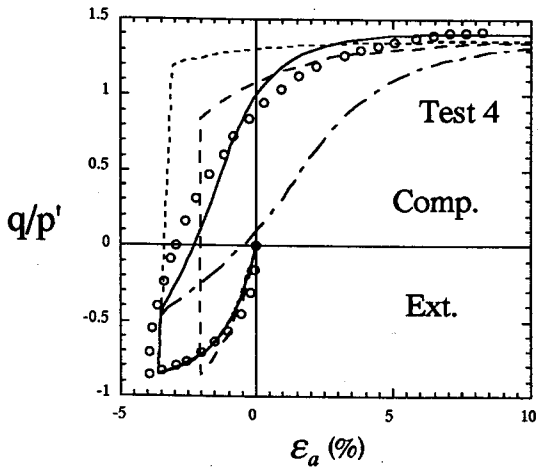

Fig 5(b): Stress ratio vs. axial strain

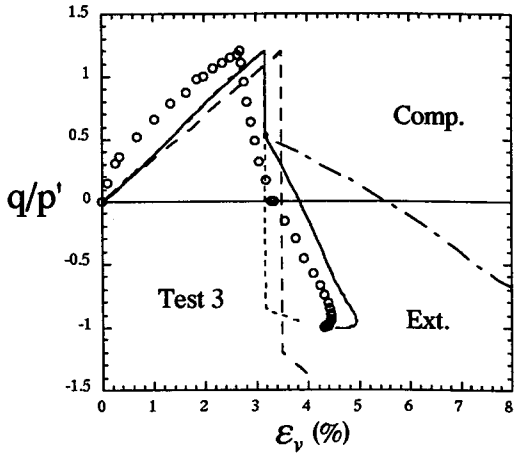

Fig 4(c): Stress ratio vs. volumetric strain

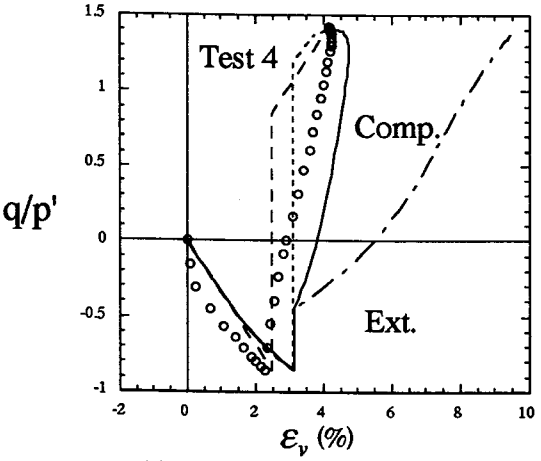

Fig 5(c): Stress ratio vs. volumetric strain

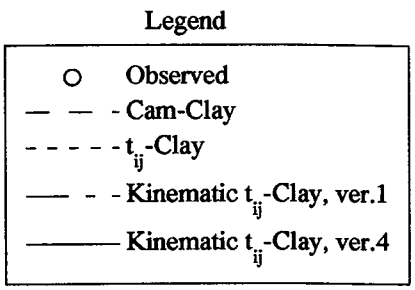

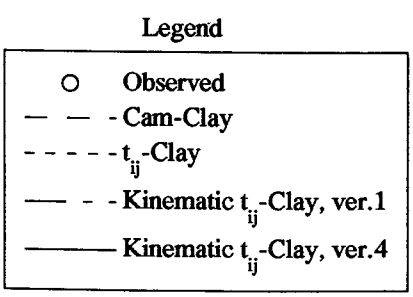

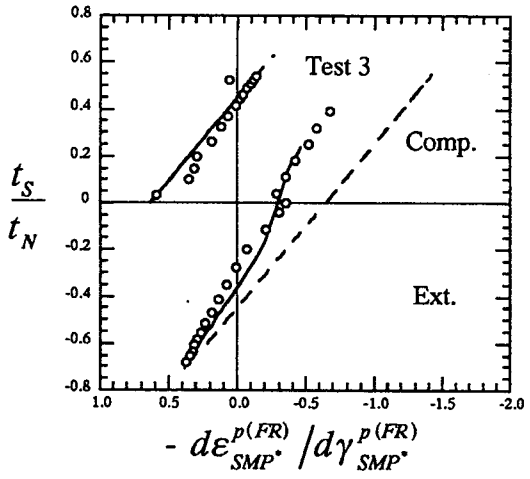

Fig 4(d): Stress-dilatancy of test 3

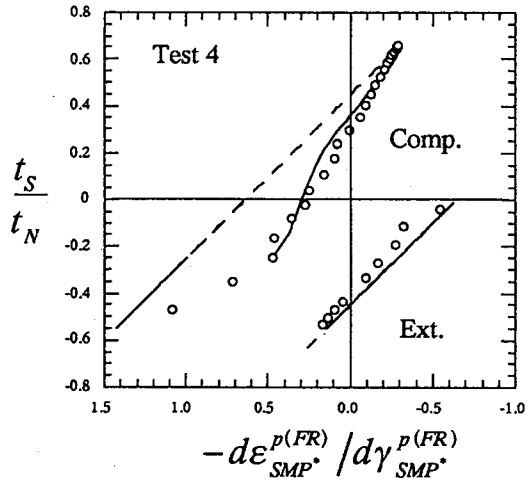

Fig 5(d): Stress-dilatancy of test 4

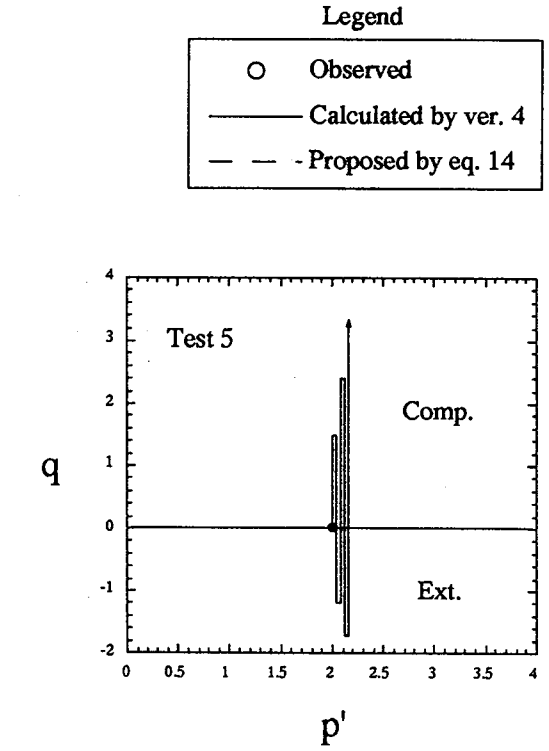

Fig 6(a): Cyclic triaxial test path

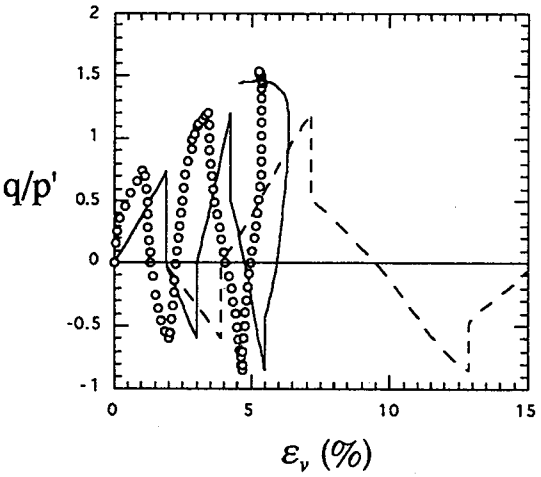

Fig 6(c): Stress ratio vs. volumetric strain

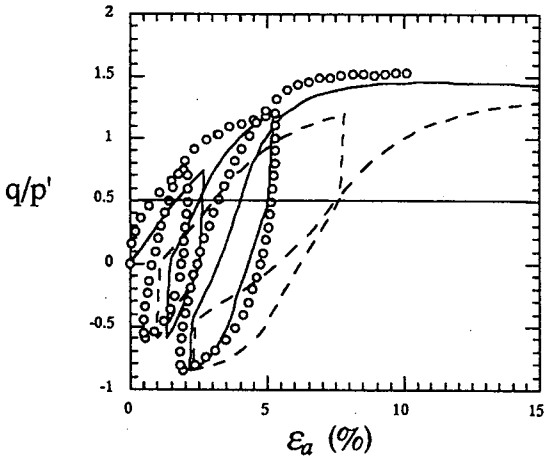

Fig 6(b): Stress ratio vs. axial strain

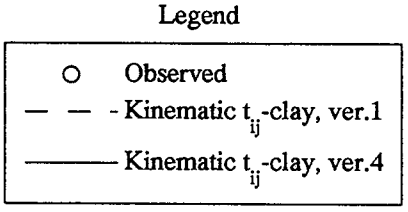

$\lambda/(1+e_0)$	5.08×10^{-2}
$\kappa/(1+e_0)$	1.12×10^{-2}
$\phi'_{(Comp.)}$	33.7°
α	0.7
ν_e	0.0
ξ	0.20
l	0.50
m	0.50
a	2.0

Table 1: Fujinomori clay parameters